

# Investigation of $^{44}\text{Ti}$ (N, P) and $^{44}\text{Ti}$ (D, 2p) Reactions in the Production of $^{44}\text{Sc}$ for Theranostic Applications

Zubaida, G.H.<sup>1</sup>, Koki, F.S.<sup>2</sup>, and Ahmad, I.<sup>3</sup>

<sup>1</sup>Department of Physics, Yusuf Maitama Sule, Federal University of Education, Kano, Nigeria

<sup>2,3</sup>Department of Physics, Bayero University Kano Nigeria

DOI: <https://doi.org/10.51584/IJRIAS.2025.100700060>

Received: 26 June 2025; Accepted: 02 July 2025; Published: 08 August 2025

## ABSTRACT

Sustainable use of nuclear medicine procedures for diagnosis and therapy of complex anomalies will continue to rely on the emergence of more radionuclides in the quest to achieve higher efficacy, higher image resolution or more efficient therapy – one of such radionuclides is Scandium-44, a positron emitter that holds the potential to propel the theranostics approach to higher levels. This paper investigates the  $^{44}\text{Ti}$  (n,p) and  $^{44}\text{Ti}$  (d,2p) reactions for the production of  $^{44}\text{Sc}$  using GEANT4, a C++ MC based simulation toolkit with a view to identify the more efficient route in terms of incident energy production cross sections. The findings show that (n,p) reactions generated higher cross sections at threshold which declines with rising neutron energy. The (d,2p) reaction despite exhibiting lower cross sections also dispose a number of isomeric states posing challenge to optimization. Excitation functions of both reactions showed good agreement with both evaluated (ENDF) and experimental EXFOR datasets. As  $^{44}\text{Sc}$  ( $t_{1/2} = 4$  h) is used for PET, and matched with  $^{47}\text{Sc}$  ( $t_{1/2} = 3.5$  d) for theranostics approach, its ability to replace Gallium ( $t_{1/2} = 68$  min) makes it possible to take the radionuclide to distant PET centers in addition to its use in planning and monitoring targeted radionuclide therapy of some radionuclides.

**Keywords:** Radionuclide, GEANT4, Optimization, Theranostics, Excitation function

## INTRODUCTION

The use of nuclear radiation techniques for non-invasive diagnosis and targeted radionuclide therapy (TRT) shall continue to play invaluable role in treatment of variety of cancers with the utilization of radiotherapeutic radiopharmaceuticals (Phillips, n.d.) which are labelled with assorted types of medically important radionuclides (Usman & Ahmad, 2022). For diagnosis, low energy gamma rays/annihilation photons are used (Volkert & Huffman, 1999) while radionuclides that emit charged particles (Auger electrons, Beta, and Alpha particles are used for therapy (Chadwick, 1995). Cancer treatment involves use of low energy dose imaging in order to extract the fundamental pre-therapy data on individual patient's bio-distribution and dosimetry of the radiopharmaceutical (Rösch et al., 2017). This is then succeeded by higher dose targeted molecular radiotherapy on the same patient based on the generated individualized data. This merger of diagnostic imaging and therapeutic treatment is now referred to as theranostic approach (Nagai et al., 2022) which is contemporarily emerging as an important concept in tailoring nuclear diagnosis and therapy to the personal specifications of patients.

The growth of interest in  $^{44}\text{Sc}$ , with a 4.00 hours half-life was due to its ability to establish high resolution imaging in PET (Müller et al., 2018). The emission characteristics of  $^{44}\text{Sc}$  which include  $\beta^+$  of 134 keV and gamma emission of 208 keV makes the radionuclide ideal for combination with vector molecules for theranostic treatment (Kumar & Ghosh, 2021). In cases where  $^{177}\text{Lu}$  or  $^{90}\text{Y}$ , both therapeutic radionuclides are paired with  $^{68}\text{Ga}$ , a PET radionuclide with 68 minute half-life, this theranostic application can now be taken to distant health facilities when  $^{44}\text{Sc}$  replaces  $^{68}\text{Ga}$  thereby increasing the emission time fourfold (Mikolajczak et al., 2021).

The current production of  $^{44}\text{Sc}$  relies on  $^{44}\text{Ti}/^{44}\text{Sc}$  generator as well as cyclotron production using up to 11 MeV proton beam irradiation of enriched  $^{44}\text{Ca}$ , a 2 hour operation that yields up to 2 GBq of activity (Choiński & Łyczko, 2021). Other routes of production also involved enriched Ti including  $^{47}\text{Ti}$  (p,a),  $^{48}\text{Ti}$  (p,na) and  $^{49}\text{Ti}$  (p,2na) reactions – these high threshold reactions are endothermic. The use of particle induced reactions on  $^{44}\text{Ti}$  for  $^{44}\text{Sc}$  production such as  $^{44}\text{Ti}$  (n,p) and  $^{44}\text{Ti}$  (d,2p) remains underexplored, this is because there is limited knowledge of particle reaction cross sections across 0 – 25 MeV range. This work hence aims to investigate the  $^{44}\text{Ti}$  (n,p) and  $^{44}\text{Ti}$  (d,2p) reactions with a view to identify the most efficient route for  $^{44}\text{Sc}$  production. Other objectives include calculation of energy dependent cross section for the reactions from which yield and optimization of production can be accomplished. The work equally aspires comparison of calculated datasets with experimental and theoretical predictions just as the simulation would unveil accuracy limitations of previous studies. Consequent recommendations it is hoped, will give way to scalable production of  $^{44}\text{Sc}$  for clinical applications.

Not a lot of studies have been reported of  $^{44}\text{Sc}$  production using Ti targets. Choinski et al (2021) reported production of  $^{44}\text{Sc}$  using two ways, either via  $^{44}\text{Ti}/^{44}\text{Sc}$  generator or directly by enriched  $^{44}\text{Ca}$  irradiation. Loveless (2020) reported  $^{44}\text{Sc}$  production from particle induced reactions on Ti while Muller et al also reported Ti/Sc generator as initially preferred route with development thereafter of natural Ca irradiation using cyclotron which yields up to 650 MBq of activity upon 1 hour of irradiation. The aim of this work is to use GEANT4 simulation in evaluating excitation functions of  $^{44}\text{Ti}(n,p)^{44}\text{Sc}$  and  $^{44}\text{Ti}(d,2p)^{44}\text{Sc}$  reactions in the low energy range of 0 – 25 MeV and subsequently determine the maximal  $^{44}\text{Sc}$  yield in the range. The work will further optimize conditions to achieve high purity of  $^{44}\text{Sc}$  for theranostic applications just as through comparing the two reaction routes seeks to decide the more efficient in terms of production energy, yield and purity.

## THEORETICAL BACKGROUND

To calculate reaction cross sections for nucleus-nucleus interactions across a broad energy spectrum, the GEANT4 toolkit incorporates the formulas developed by Tripathi, Kox, Sihver, and Shen (Cao *et al.*, 2009). These formulas are parameterized to account for theoretical aspects such as Coulomb corrections, asymmetric proton and neutron numbers, Pauli blocking, and other factors (Folger *et al.*, 2003). This parameterization can be generally expressed as

$$\sigma_R = \pi r_0^2 \left( A_p^{\frac{1}{3}} + A_T^{\frac{1}{3}} + \delta \right)^2 \left( 1 - \frac{Bc}{E_{cm}} \right) \quad (1)$$

Where  $r_0$  is the reduced nuclear radius parameter and is energy independent,  $A_p$  and  $A_T$  are the mass numbers of projectile and target respectively and  $E_{cm}$  is the colliding system centre of mass energy in MeV,  $\delta$  is either energy dependent or independent parameter. while the last term of the equation is the Coulomb interaction term (with Coulomb barrier  $Bc$ )(Rehman *et al.*, 2011).

The Q-value of a nuclear reaction is the net energy change during the reaction. It is calculated as:

$$Q = \{ (A_T + A_p) - (A_r + A_e) \} \quad (2)$$

where  $A_r$  is the mass of product nuclei and  $A_e$  is the mass of ejectile. The threshold ( $T_m$ ) energy for charged-particle reactions depends on the Q-value and is higher than Q-value due to the Coulomb barrier. For a reaction to occur, the incident particle must have energy greater than or equal to the reaction threshold.

$$T_m = Q \frac{A_p + A_r}{A_r} \quad (3)$$

## METHOD

This paper employed Geometry ANd Tracking version 4 (GEANT4) toolkit, CMake 3.3, Visual Studio 2022, Microsoft Excel, ENDF and EXFOR database libraries to model neutron, deuteron particles interactions in  $^{44}\text{Ti}$  target. The selected physics list was QGSP\_BERT\_HP which combines three physics processes namely Quark Gluon String Parton, Bertini cascade and High Precision processes, to simulate different reaction stages, from initial nucleon interactions to final de-excitation. The target geometry was modeled as cubical slab to minimize particle self-absorption effects. A monoenergetic particle beam (neutrons and deuterons) was configured with energies ranging from 0 to 25 MeV. The maximum energy selection was based on the criteria that theranostic candidate nuclides must be produced using low energy reactions achievable in common accelerators/cyclotrons affordable to hospitals. QGSP\_BERT\_HP physics list was used to evaluate the reaction channels and the reaction cross sections for theranostic isotopes production. One spectacular advantage of this simulation type over purely mathematical models is its capability to model geometries of varying complexity in addition to its flexibility and wealth of choice from a constellation of theoretical and data driven models

The output displayed reaction cross sections and other parameters. Multiple runs were conducted for each configuration to ensure reproducibility and minimize random fluctuations. Output data was processed using MS Excel ensuing the evaluation of excitation functions of the reactions. Simulated reaction cross-sections were compared against experimental datasets EXFOR and evaluated datasets ENDF from Nuclear Data Section (NDS) of the IAEA, for comparison and validation of simulation accuracy. The outputs tolerate a cost effective test of radioisotope production set-ups just as it identifies production of undesirable contaminant radioisotope species produced via competing reaction channels which may impact both diagnostic and therapeutic procedures. This acquiesces for evaluation of the potential impurities in the produced theranostic radiopharmaceutical. The simulation by the same token makes it possible to evaluate the corollaries of misalignment of the particle beams on the production yield as it allows the user to alter the parameters of the particle beam.

In the present work, all uncertainties were considered uncorrelated hence, quadratically summed according to error propagation laws to get total errors. Furthermore, while some of the error sources are common to all data, others affect individual reactions. Yet, the cumulative uncertainties: statistical uncertainties of number of events (0.5 – 5%), systematic uncertainty of the beam flux (~6%), the uncertainty of number particles generated (4 – 6%) and the uncertainty of Q-value evaluation (3%). The overall uncertainties of the cross section evaluation were in the range of 8 – 15%, and in GEANT4 code, the Analysis Manager class automatically records such errors.

## RESULTS

The excitation functions of  $^{44}\text{Ti}(\text{d},2\text{p})$  and  $^{44}\text{Ti}(\text{n},\text{p})$  reactions for the production of  $^{44}\text{Sc}$  is presented in figures I and II respectively

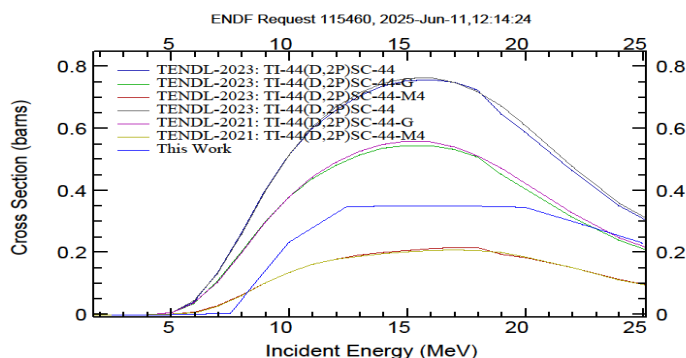


Figure I – Excitation function of  $^{44}\text{Ti}(\text{d},2\text{p})$   $^{44}\text{Sc}$  reaction

In Figure I the excitation function shows good agreement with evaluated data libraries including TENDL – 2023 (Koning *et al.*, 2023), and TENDL – 2021( Koning *et al.*, 2021) especially in the low energy tail but in mid energies it showed a little stability around the equilibrium region possibly as a result of statistical error. At energies from 20 MeV there is remarkable agreement as well as convergence with TENDL – 2023 values. Further, our findings show the (d,2p) reaction achieves maximum cross section at 20 MeV making it an essentially high energy reaction compared to the (n,p) channel which shows peak cross section of 0.5874 barns at 5 MeV implying it as more favorable channel with regard to the need for a theranostic radionuclide to come from a low energy reaction.

Q-value, is the net energy change in a reaction is a very important factor and plays a big role in determining reaction feasibility of different channels. In this perspective the (n,p) channel with Qvalue of 1.0107 MeV has threshold of 2.5 MeV whence its Q-value points its exoergic reaction and more favored to occur and produce more energetic ejectiles. The (d,2p) rote on the other hand has Qvalue of -1.1722 MeV making it thus endoergic requiring to absorb energy from incident deuterons before achieving threshold of 7.5 MeV and hence produces ejectiles less energetic than the (n,p) channels.

The (d,2p) reaction is inundated with several metastable variants of  $^{44}\text{Sc}$  (as seen in Figure III) with each in different excitation energy – these include  $^{44\text{m}}\text{Sc}$  with 271.240 keV excitation energy and half-life of 5.1 days. This variant decays by Auger electron emission while its internal conversion of electrons can play a therapeutic role by causing localized DNA damage at cellular levels.  $^{44\text{m1}}\text{Sc}$  has 146.191 keV excitation energy and half-life of  $51 \pm 0.3 \mu\text{s}$  and decays by isomeric transition (IT).  $^{44\text{m2}}\text{Sc}$  is another substantive variant with 132.226 keV excitation energy and half-life of  $154.8 \pm 0.8 \text{ ns}$  and decays to ground state by IT. Further, several other variants may be found at intermediate excited levels, but they usually decay by transition to other metastable states or ground state. On the whole, the production of  $^{44\text{m}}\text{Sc}$  which can serve as theranostic due to its emission characteristics presents a more advantageous potential of the (d,2p) reaction especially for the fact that the other metastable variants can be optimized using post irradiation timing leaving  $^{44\text{m}}\text{Sc}$  which can be further optimized using excitation function.

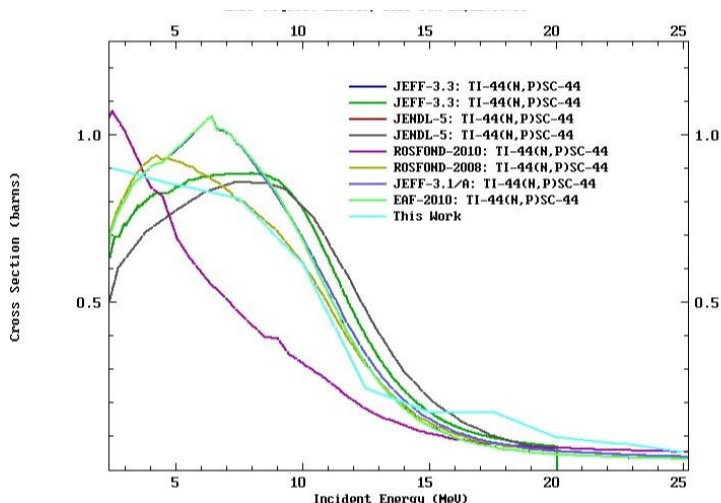


Figure II – Excitation function of  $^{44}\text{Ti}(\text{n,p})$   $^{44}\text{Sc}$  reaction

Figure II displays the excitation function of  $^{44}\text{Ti}(\text{n,p})$  reaction in good agreement with evaluated nuclear datafiles JEFF 3.3(Lunev *et al.*, 1992), JENDL-5 (Koning *et al.*, 2021), ROSFOND (2018), ROSFOND (2010) and EAF (2010) (Koscheev 2010). There is peak cross section at low energies of the excitation functions which is a signature of neutron reactions. Hence the exhibition of high energy tail following the usual compound nucleus formation in the low energy region of the reaction. This trend implies that a high yield of  $^{44}\text{Sc}$  would be achieved in the low energy region of the reaction which makes the reaction more favourable than (d,2p) reaction as theranostic nuclides need to be products of low energy reactions.

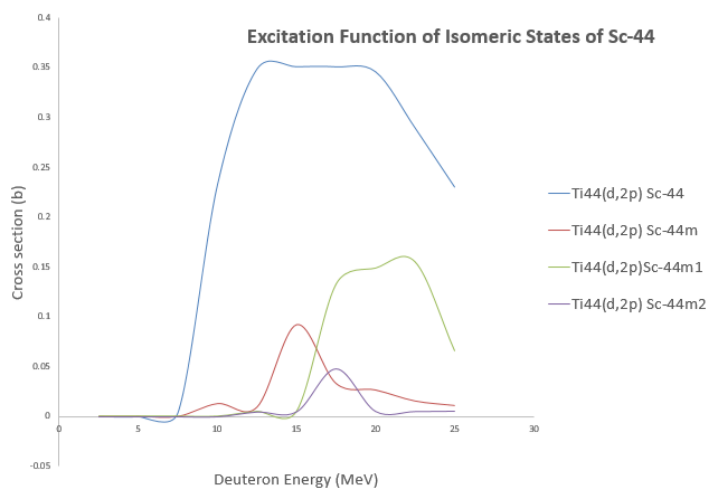


Figure III – Excitation function of competing channels of  $^{44}\text{Ti}(d,2p)^{44}\text{Sc}$  reaction

Figure III shows the excitation function of reaction channels that compete with  $(d,2p)^{44}\text{Sc}$  reaction and it is evident that these channels that yield  $^{44}\text{Sc}$  isomers,  $^{44\text{m}}\text{Sc}$ ,  $^{44\text{m1}}\text{Sc}$  and  $^{44\text{m2}}\text{Sc}$  exhibit comparatively much lower excitation function than stable  $^{44}\text{Sc}$ .  $^{44\text{m}}\text{Sc}$ , demonstrated threshold value of 10 MeV while  $^{44\text{m1}}\text{Sc}$  and  $^{44\text{m2}}\text{Sc}$  show common threshold of 12.5 MeV. As ground state  $^{44}\text{Sc}$  has threshold of 7.5 MeV, it follows then that the energy region between 7.5 MeV and 10 MeV shows the best chance of producing high purity  $^{44}\text{Sc}$  from the  $(d,2p)$  reaction.

The  $(n,p)$  reaction has the advantage of having low threshold and high cross sections at low energies but its main drawback is that neutron reactions conform usually with reactor production albeit some accelerators support neutron reactions. The  $(d,2p)$  channel on the other hand is well supportable with small cyclotrons affordable to hospitals but its high threshold and maximal cross sections at high energies almost impedes its theranostic properties as the approach needs low energy produced nuclides.

Gamma rays' emission that accompanies both reactions is compared in Table 1 below which shows the  $(d,2p)$  reaction maintaining high energy gamma at low energy tail of the reaction and continues to rise throughout the reaction.  $(n,p)$  reaction however showed low energy gamma especially at 5 MeV where  $^{44}\text{Sc}$  production cross section is maximum indication that neutron interactions with  $^{44}\text{Ti}$  target yields  $^{44}\text{Sc}$  with low gamma energy which is preferred as theranostic radionuclide production requires.

Table 1 – Comparison of Gamma emission as incident energy function in  $^{44}\text{Ti}(n,p)$  and  $^{44}\text{Ti}(d,2p)$  reactions

Incident energy (MeV)	$^{44}\text{Ti}(n,p)^{44}\text{Sc}$ ( $E_\gamma$ )	$^{44}\text{Ti}(d,2p)^{44}\text{Sc}$ ( $E_\gamma$ )
2.5	587.09 KeV	1.0595 MeV
5	931.52 KeV	1.0795 MeV
7.5	1.3349 MeV	1.1153 MeV
10	1.6836 MeV	1.2119 MeV
12.5	1.8651 MeV	1.154 MeV
15	1.8171 MeV	1.2624 MeV
17.5	1.7273 MeV	1.3279 MeV
20	1.8752 MeV	1.4269 MeV



22.5	1.977 MeV	1.6353 MeV
25	2.095 MeV	1.8254 MeV

In Table 1 the gamma energy emission of (n,p) and (d,2p) reactions is presented at each energy level of the reaction range and it shows increase in gamma emission with increasing incident energy in both reactions. However, as low gamma emission is considered essential in production of theranostic radionuclides, the (n,p) reaction shows lower gamma at low energy region of the reaction compared to (d,2p) while at higher energies the former also shows comparatively higher gamma energy values.

Table 2 – Comparison of Mean energy of  $^{44}\text{Sc}$  product as incident energy function in  $^{44}\text{Ti}$  (n,p) and  $^{44}\text{Ti}$ (d,2p) reactions

Incident energy (MeV)	$^{44}\text{Ti}(\text{n,p})$ $^{44}\text{Sc}$ (KeV)	$^{44}\text{Ti}(\text{d,2p})$ $^{44}\text{Sc}$
2.5	111.72	-
5	201.21	-
7.5	251.93	332.56 KeV
10	356.04	527.17 KeV
12.5	431.21	766.19 KeV
15	416.15	755.12 KeV
17.5	518.61	1.076 MeV
20	842.04	1.2579 MeV
22.5	830.69	1.2957 MeV
25	875.0	1.4577 MeV

Table 2 shows the average mean energy of  $^{44}\text{Sc}$  produced at each energy level for both the (n,p) and (d,2p) channels. The latter shows increasing mean energy as incident deuteron energy rises while the low energy region of (n,p) channels shows comparably lower mean ejectile energy. The optimal mean energy of  $^{44}\text{Sc}$  is 134 keV and as the (n,p) reaction at 5 MeV gives mean energy of 201.21 keV, the route is indicated as more efficient as its energy is close to the optimal requirement.

Table 3 – Summary of Comparison between  $^{44}\text{Ti}(\text{n,p})$   $^{44}\text{Sc}$  and  $^{44}\text{Ti}(\text{d,2p})$   $^{44}\text{Sc}$  reactions

Parameter	$^{44}\text{Ti}(\text{n,p})$ $^{44}\text{Sc}$	$^{44}\text{Ti}(\text{d,2p})$ $^{44}\text{Sc}$
Reaction type	Exothermic	Endothermic
Threshold Energy	< 2.5 MeV	7.5 MeV
Mean Gamma emission energy at Threshold	587.09 keV	1.2624 MeV
Maximum cross-section	0.851 b	0.3507 b

Energy for Maximum cross-section	5 MeV	15 MeV
Isomeric States	$^{44}\text{Sc}$ $^{44\text{m}}\text{Sc}$	$^{44}\text{Sc}$ $^{44\text{m}}\text{Sc}$ [271.240] keV $^{44\text{m}1}\text{Sc}$ [146.191] keV $^{44\text{m}2}\text{Sc}$ [132.226] keV
Optimization type	Excitation function at 10 MeV $\rightarrow$ 7.5 MeV	Post irradiation Timing
Validation	Excitation function in good agreement with TENDL 2021 and TENDL 2023	Excitation function in good agreement with JEFF 3.3, JENDL 5, ROSFOND 2008, ROSFOND 2010, JEFF-3 and EAF 2010

Table 3 summarized the Comparison between  $^{44}\text{Ti}(\text{n,p})$   $^{44}\text{Sc}$  and  $^{44}\text{Ti}(\text{d},2\text{p})$   $^{44}\text{Sc}$  reactions. All Validations were evaluated data from ENDF-NDS library. Within this research limit there is no experimental data to compare with this work.

## CONCLUSION & RECOMMENDATION

The excitation function of  $^{44}\text{Ti}(\text{n,p})$  and  $^{44}\text{Ti}(\text{d},2\text{p})$  reactions have been investigated using GEANT4 simulation toolkit, according to our findings the (n,p) reaction achieves maximum cross section at 5 MeV achieving low gamma energy at the same energy level while the (d,2p) reaction reached peak cross section at 15 MeV. The latter reaction displayed several isomeric states of excited  $^{44}\text{Sc}$  forms in various energy states of which  $^{44\text{m}}\text{Sc}$  is predominant and is regarded as theranostic due to its half life and decay mode. Based on the findings, and in line with the objectives of this study, the (n,p) reaction appears to be more promising in production of  $^{44}\text{Sc}$ , positron emitter with 4 hour half-life useful in theranostic imaging. This assertion is based further on the low gamma emission as well as low production energy – two criteria needed as preconditions for a radionuclide to be a true theranostic. The low production energy is important to allow small health facilities to produce the radionuclide using small cyclotrons within the facility. Moreover, as this work focuses more on low energy reactions, it also underscores the fact that  $^{44}\text{Sc}$  clenches great potential for future as a novel positron emitting nuclide for theranostic diagnostic imaging and therapy monitoring. Titanium has a comparatively low cost and can be afforded by most radiopharmaceutical entities hence, the investigation of reactions of low energy profile on enriched isotopic targets has and shall continue to facilitate development of positron emitting nuclides production routes for small cyclotrons in local hospitals.

## REFERENCES

- Chadwick, M. B. (1995). Medical and industrial applications of nuclear reaction physics. Acta Physica Hungarica New Series Heavy Ion Physics, 2(3–4), 333–346. <https://doi.org/10.1007/BF03055117>
- Choiński, J., & Lyczko, M. (2021). Prospects for the production of radioisotopes and radiobioconjugates for theranostics. Bio-Algorithms and Med-Systems, 17(4), 241–257. <https://doi.org/10.1515/bams-2021-0136>
- Koning, A., Hilaire, S., & Goriely, S. (2023). Talys-2.0. In TALYS-2.0 Simulation of nuclear reactions.
- Koning, A. J., Rochman, D., Sublet, J., Dzysiuk, N., Fleming, M., & Marck, S. Van Der. (2021). TENDL : Complete Nuclear Data Library for Innovative Nuclear Science and Technology. Nuclear Data Sheet, 155, 1–55.
- Koscheev V.N. (2010) The European Activation File: Cross section Library - UKAEA FUS 486
- R. A. Forrest, J. Kopecky and J-Ch Sublet. (2003).
- Kumar, K., & Ghosh, A. (2021). Radiochemistry, production processes, labeling methods, and immunopet imaging pharmaceuticals of iodine-124. Molecules, 26(2).

<https://doi.org/10.3390/molecules26020414>

8. Lunev, V. P., Kurenkov, N. V., Malinin, A. B., Masterov, V. S., & Shubin, Y. N. (1992). AN Analysis Of Reaction Cross-Section Calculational Methods For The Production Of Medical Radioisotopes V.P.Lunev,. 05, 609–610.
9. Mikolajczak, R., Huclier-Markai, S., Alliot, C., Haddad, F., Szikra, D., Forgacs, V., & Garnuszek, P. (2021). Production of scandium radionuclides for theranostic applications: towards standardization of quality requirements. In *EJNMMI Radiopharmacy and Chemistry* (Vol. 6, Issue 1). <https://doi.org/10.1186/s41181-021-00131-2>
10. Müller, C., Domnanich, K. A., Umbricht, C. A., & Van Der Meulen, N. P. (2018). Scandium and terbium radionuclides for radiotheranostics: Current state of development towards clinical application. *British Journal of Radiology*, 91(1091). <https://doi.org/10.1259/bjr.20180074>
11. Nagai, Y., Kawabata, M., Hashimoto, S., Tsukada, K., Hashimoto, K., Motoishi, S., Saeki, H., Motomura, A., Minato, F., & Itoh, M. (2022). Estimated Isotopic Compositions of Yb in Enriched <sup>176</sup>Yb for Producing with High Radionuclide Purity by <sup>176</sup>Yb ( d , x ) <sup>177</sup>Lu. 044201, 1–10. <https://doi.org/10.7566/JPSJ.91.044201>
12. Phillips, R. (n.d.). The University of New Mexico Correspondence Continuing Education Courses for Nuclear Pharmacists and Nuclear Medicine Professionals Production of Medical Radionuclides.
13. Rehman, S. U., Mirza, S. M., Mirza, N. M., & Siddique, M. T. (2011). GEANT4 simulation of photo-peak efficiency of small high purity germanium detectors for nuclear power plant applications. *Annals of Nuclear Energy*, 38, 112–117. <https://doi.org/10.1016/j.anucene.2010.08.010>
14. Rösch, F., Herzog, H., & Qaim, S. M. (2017). The beginning and development of the theranostic approach in nuclear medicine, as exemplified by the radionuclide pair <sup>86</sup>Y and <sup>90</sup>Y. *Pharmaceuticals*, 10(2). <https://doi.org/10.3390/ph10020056>
15. Usman, A. R., & Ahmad, A. A. (2022). Evaluation of <sup>67</sup>Ga Cross-sections Using Exifon Code For Medical Applications. *FUDMA Journal of Sciences (FJS)*, 6(3), 113–118.
16. Volkert, W. A., & Huffman, T. J. (1999). Therapeutic radiopharmaceuticals. *Chemical Reviews*, 99(9), 2269–2292. <https://doi.org/10.1021/cr9804386>